Contents lists available at ScienceDirect

International Journal of Psychophysiology

journal homepage: http://ees.elsevier.com

Asymmetric effects of graspable distractor disks on motor preparation of successive grasps: A behavioural and event-related potential (ERP) study

Stefano Uccelli [a,*], Letizia Palumbo [b], Neil Harrison [b], Nicola Bruno [a]

[a] University of Parma, Italy
[b] Liverpool Hope University, United Kingdom of Great Britain and Northern Ireland

ARTICLE INFO

Keywords
Perception
Action
Grasping
Motor preparation
Two-visual-systems hypothesis
Lateralized readiness potentials

ABSTRACT

There is evidence that seeing a graspable object automatically elicits a preparatory motor process. However, it is unclear whether this implicit visuomotor process might influence the preparation of a successive grasp for a different object. We addressed the issue by implementing a combined behavioural and electrophysiological paradigm. Participants performed pantomimed grasps directed to small or large disks with either a two (pincer) or a five-finger (pentapod) grip, after the presentation of congruent (same size) or incongruent (different size) distractor disks. Preview reaction times (PRTs) and response-locked lateralized readiness potentials (R-LRPs) were recorded as online indices of motor preparation. Results revealed asymmetric effects of the distractors on PRTs and R-LRPs. For pincer grip disks, incongruent distractors were associated with longer PRTs and a delayed R-LRP peak. For pentapod grip disks, conversely, incongruent distractors were associated with shorter PRTs and a delayed R-LRP onset. Supporting an interpretation of these effects as tapping into motor preparation, we did not observe modulations of stimulus-locked LRP's (sensitive to sensory processing), or of the P300 component (related to reallocating attentional resources). These results challenge models (i.e., the "dorsal amnesia" hypothesis) which assume that visuomotor information presented before a grasp will not affect how we later perform that grasp.

1. Introduction

We effortlessly grasp objects many times every day, but grasping involves non-trivial problems of motor control. For instance, the hand must be configured before contact, and in this a key role is played by the object size as this critically constrains which fingers will be involved. For a small object, such as a peanut, we will typically use a thumb-index opposition grip ('pincer grip'). For a larger object, such as an apple, we will instead use all five fingers, with the thumb opposing the other four ('pentapod grip'). In both cases, however, the hand will approach the object quickly, open the required amount, and finish the movement by closing the digits on the aimed contact points on the object (Jeannerod, 1981; Marteniuk et al., 1990). Despite a large literature (see Smeets et al., 2019), preparatory processes involved in this remarkably efficient motor behavior are not fully understood. For instance, it is unclear whether a first motor representation can affect a second, successive motor program. Using a sequential paradigm, we investigated whether, and how, a first motor representation elicited by a graspable object affects the preparation of a second motor program aimed at grasping a different object. The theoretical backdrop of our research question lies in two concepts: affordances and visuomotor priming.

The term *affordance* (Gibson, 1979) refers to the direct perception of potentialities for action. Although the notion has been debated (de Wit et al., 2017; Chong and Proctor, 2020), a common prediction is that object observation activates motor representations even if no action will be carried out. Viewing a graspable object, for instance, automatically activates an internal representation of the potential grasp. Evidence supporting this prediction is provided by studies on monkeys (Jeannerod et al., 1995; Murata et al., 1997; Maranesi et al., 2014), as well as behavioural (Chao and Martin, 2000; Tucker and Ellis, 1998, 2004), imaging (Anderson et al., 2002; Grèzes and Decety, 2002), and TMS (Buccino et al., 2009; Grèzes et al., 2003) studies on humans. However, this literature is not directly concerned with the issue of possible effects of such representations on subsequent performed actions. Evidence relevant to this issue is instead provided by visuomotor priming tasks (Craighero et al., 1996; Craighero et al., 1998). In these tasks, reaction times are shorter (i.e. benefits) or longer (i.e. costs) depending on whether a feature of the target stimulus (e.g., its orientation) is congruent or incongruent with the corresponding fea-

* Corresponding author.
E-mail address: stefano.uccelli@studenti.unipr.it (S. Uccelli)

https://doi.org/10.1016/j.ijpsycho.2020.10.007
Received 23 April 2020; Received in revised form 29 July 2020; Accepted 20 October 2020
Available online xxx
0167-8760/

ture of an initial prime (see Craighero et al., 1996, 1998). Similar findings have been replicated and extended in other studies (Hesse et al., 2008; Roche and Chainay, 2013; Seegelke et al., 2016). It has also been argued, however, that visuomotor priming effects may not occur at the level of motor representations and could well involve semantic rather than motor interactions (Cant et al., 2005; but see, Hesse et al., 2008, Seegelke et al., 2016).

Thus, empirical work on affordances and on visuomotor priming indicates that a motor representation might be automatically elicited when seeing an object that affords appropriate action potentialities. We call this the *automatic visuomotor encoding* hypothesis. However, it remains unclear whether such representations can feed later motor processes. For instance, they might be confined to the seen object in space and especially in time, such that they will quickly decay as soon as new processing is called for. Indeed, it has been proposed that object-directed actions rely only on online sensory information. This *real time motor control* view (Westwood and Goodale, 2003) is a key feature of the influential two-visual-systems hypothesis (TVSH, Goodale and Milner, 1992; Milner and Goodale, 2008; Milner, 2017). According to the TVSH, the ventral stream codes visual information to generate representations that remain invariant under contextual changes allowing object recognition ("vision-for-perception"). Instead, the dorsal stream processes information relevant for the online control of goal-directed actions ("vision-for-action"). Critically for the purposes of the current paper, vision-for-action is assumed to code "here-and-now" relationships between an object and the action's effector, disregarding how the object relates to its context, especially in time (i.e., "dorsal amnesia"; Schenk and Hesse, 2018).

In this paper, we challenged real time motor control investigating whether motor preparation for grasping an object is affected by a previously elicited motor representation for grasping a different object. Imagine the following situation. You see a peanut. Immediately afterwards, you see an apple, which you have to grasp. Will the peanut (which affords a *pincer* grip), affect the motor preparation for grasping the apple (which affords a *pentapod* grip)? If object observation automatically elicits an (implicit) motor representation (i.e., if there is automatic visuomotor encoding), one could expect that this representation might affect the successive action. Support for this prediction is provided by a study on the Uznadze illusion in action (Uccelli et al., 2019). In this illusion, the same object is perceived as smaller when preceded by a larger object and vice versa (Uznadze, 1966). This temporal size contrast yields strong perceptual effects in haptics (Kappers and Bergmann-Tiest, 2014), in vision-for-perception (Bruno et al., 2018), and in a vision-for-action task (Uccelli et al., 2019).

Critical for the purpose of the current paper, there is evidence that the effect of the Uznadze illusion might already occur at the level of motor preparation (Pisu et al., 2020). In this work, small, medium, and large disks were used both as distractors and as targets. Small disks were associated with 'pincer grips' (thumb-index opposition), medium disks with 'tripod grips' (thumb vs index and middle), and large disks with 'pentapod grips' (all five fingers). The design involved congruent (baseline) or incongruent (differently sized targets and distractors) conditions. After seeing a distractor, participants grasped a target in open-loop conditions after a discretional preview time window. This determined the preview reaction time (PRT), i.e. the time spent observing the target before movement onset. Results indicated that incongruent distractor-target pairs were generally associated with longer PRTs, but differences were reliable only when participants grasped small targets after the presentation of larger distractors. When large targets were grasped after the presentation of smaller distractors, PRTs could not be reliably differentiated from the relevant baseline. Pisu et al. (2020) interpreted this pattern as reflecting an asymmetric generalization of precision between the two motor programs. They suggested that the implicit pre-activation of less precise grips (i.e., pentapod) yielded longer PRTs as the precision parameter had to be updated to perform a more demanding grip (i.e., pincer). Conversely, the higher precision associated with a pincer grip generalized to the preparation of a successive, less precise grip. Here we sought to corroborate this interpretation by investigating into the temporal dynamics of brain activity related to the preparation of grasping.

1.1. Testing real-time control with ERPs: rationale and predictions

Components of ERPs can provide temporal markers for specific brain processes. In motor preparation, one such marker is the lateralized readiness potential (LRP). The LRP is a slow negative ERP modulation which unfolds well before movement initiation from one of the motor cortices (Gratton et al., 1988; Smulders and Miller, 2012). LRPs can be measured with reference to stimulus onset (stimulus-locked lateralized readiness potential, or S-LRP), or to action initiation (response-locked, or R-LRP). The former reflects stimulus processing, while the latter reflects motor preparation (Smulders and Miller, 2012; Leuthold et al., 1996; Osman et al., 1992). In addition, stimulus processing in preparation for an action recruits attentional resources. The P300 is a positive ERP component that appears after a task-relevant stimulus (Sutton et al., 1965). Although the issue is still debated (Verleger, 1997), P300 amplitude is generally believed to reflect "context updating" in terms of attentional costs (Donchin and Coles, 1988), while P300 latency (i.e., the time between stimulus onset and P300 amplitude peak) is believed to reflect evaluation and categorization processes, independent of response selection and execution (Segalowitz et al., 1997; Magliero et al., 1984).

By using LRPs, we aimed to extend previous work on temporal dynamics within cortical networks for motor preparation. Specifically, we aimed to assess how an implicit motor representation might affect the preparation of an explicit successive grasp. If PRTs for grasping a target are modified by the presentation of incongruent distractors (as reported by Pisu et al., 2020), and if this effect occurs at the level of motor preparation (as hypothesized again by Pisu et al.), then corresponding ERP modulations should be observed in R-LRP's, but not in S-LRP or P300 components.

2. Methods

2.1. Power analysis

To determine the adequate sample size, we conducted an a-priori power analysis. First, we asked what would be a meaningful effect size for the present research. Pisu et al. (2020) reported that non-transformed PRTs group averages of 16 participants in the baseline (congruent) conditions were 890 and 830 ms for pincer and pentapod grips, respectively. In the corresponding test (incongruent) conditions, group averages were 990 and 860 ms (i.e., incongruent distractor-target pair of disks revealed effect sizes of ≈100 and 30 ms). Taking these results as a starting point, we assessed power under three hypothetical scenarios involving effect sizes equal to 70%, 60%, or 50% of effects found by Pisu and colleagues. Power estimates were obtained by simulating and then modelling 10,000 independent experiments using the *simr* package in R (Green and MacLeod, 2016), with increasing numbers of participants. We selected $n = 22$ as power estimates were 0.99, 0.95, and 0.85 for the three scenarios, respectively. Finally, we assumed that this sample size would be adequate to detect differences in ERP signatures as there is no a-priori reason to predict larger inter-participant variability than in PRTs, especially given that we registered LRP signals in

60 trials for each experimental condition when it is usually recommended that 40–50 trials suffice to derive satisfactory waveforms (Eimer, 1998). Details of the power simulations are provided in the Open Analysis document (https://osf.io/yvsg5/).

2.2. Participants

Twenty-two members of the Liverpool Hope University community (9 females and 13 males, mean age = 23.9, range: 19–37) participated. All were right-handed, had normal or corrected-to-normal vision, no history of neurological disease, and were unaware of the purpose of the study. Seventeen undergraduate students volunteered by booking weekly slots on the SONA recruitment system and received course credits for participating in the study; the other five were faculty members of the Department of Psychology recruited by the first author. The only inclusion criterion was that they be right-handed. One additional volunteer was excluded from the analysis as she turned out to be left-handed after testing had already been completed.

2.3. Ethics

All participants signed a written informed consent form before participating and were debriefed as to the purposes of the study after participation. The study received approval from the Psychology Research Ethics Committee of Liverpool Hope University and was conducted in accordance with the ethical standards of the Code of Ethical Principles for Medical Research Involving Human Subjects of the World Medical Association (Declaration of Helsinki), as well as the Code of Ethics and Conduct of the British Psychological Society.

2.4. Stimuli

Stimuli were generated in MATLAB (2015b, The MathWorks, Natick, MA, USA) using the Psychophysics toolbox extension, version 3.0 (Brainard, 1997). They consisted of a small and a large white disk having diameters of 38 and 380 pixels, respectively (corresponding approximately to 10 and 100 mm). They were presented at the center of the computer screen surrounded by a black background. The on-screen luminance of the disks and background were approximately 95 and 0.5 cd/m^2. Stimuli were presented on a 17 in. monitor controlled by a computer running the Windows XP operating system.

2.5. Task

Participants pantomimed a reach-to-grasp movement with their right hand towards a small or large target disk, after a discretional preview time window. Disks were paired with a different type of grasp, considered as the most appropriate grasp for an object having that size. Pairings were defined based on the taxonomy proposed by Feix et al. (2015). Thus, participants were instructed and trained to grasp the small disk with a pincer grip (thumb and index opposition) and the large disk with a pentapod grip (all five fingers).

2.6. Design

The design resulted from crossing two within-participant independent variables: the distractor (two levels, see Stimuli section) and target (also two levels) sizes. This yielded four experimental conditions, each consisting of one distractor - target pair. Two of these pairs involved distractors and targets having the same size (congruent, baseline). The other two involved distractors and targets having different sizes (incongruent, test). The experimental design is illustrated in Fig. 1. Given our rationale, we compared each incongruent pair with its appropriate baseline. Thus, we compared responses to small targets preceded by large distractors to the baseline involving small targets preceded by small distractors. Similarly, we compared responses to large targets preceded by small distractors to baselines involving large targets preceded by large distractors. To minimize participant fatigue, the experiment was divided into 6 blocks separated by 2–3 min pauses, giving the participant a brief break while the experimenter prepared the next block. Each pair was presented 10 times, yielding a total of 40 fully randomized trials per block. Thus, over the 6 blocks we collected measures from 240 trials, (60 distractor - target trials per pair per participant).

2.7. Procedure

The participant sat on a comfortable chair in a lightly lit room. A keyboard was placed on the table in front of the participant. The center of the spacebar and the participant's midline were aligned with the center of the computer screen. The spacebar was placed at exactly 23 cm from the computer screen, corresponding to a viewing distance of approximately 50 cm. The experiment began with a verbal explanation, followed by twelve randomly chosen practice trials. When necessary, practice trials were repeated additional times until the participant was comfortable with the trial sequence. A written reminder of the instructions was also displayed on the screen before starting the experiment.

The trial sequence is illustrated in Fig. 2. At the beginning of each trial, a red cross appeared at the center of the computer screen to signal the participant to press the spacebar: this caused the presentation of the distractor disk on the center of the screen. The participant was required to maintain fixation on the screen center without taking any action (distractor phase). The distractor lasted for 3 s and was followed by a go-signal informing the participant to go on with the trial. The participant pressed the spacebar again, but this time held it down as long as needed to observe the target disk and prepare the appropriate grip. At this spacebar press, the target disk

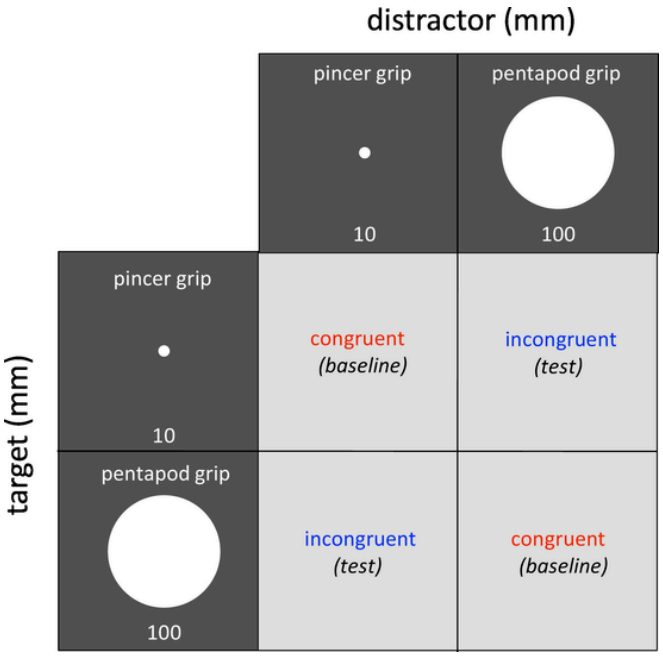

Fig. 1. The four experimental conditions. Participants were trained to perform a simulated pincer (index-thumb opposition) or pentapod (thumb - other four fingers) grip, respectively on a small (10 mm diameter) or large (100 mm diameter) target disk. Congruent or incongruent distractors were presented before tests.

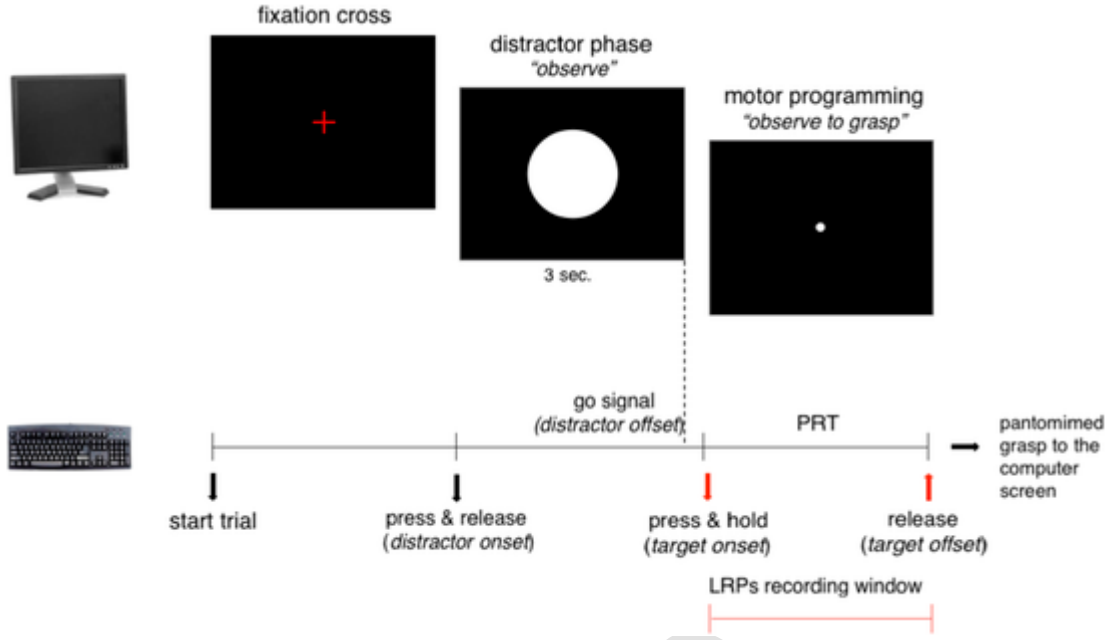

Fig. 2. Structure of trials. The fixation cross and stimuli were presented on a monitor. The space key on a computer keyboard was used to record keypresses and releases.

was displayed on the center of the computer screen (target onset), recording of the PRT for the current trial was initiated, and MATLAB issued a trigger to the EEG marking the onset. Then, once ready to perform the appropriate grip (i.e., the pincer grip for small disks and the pentapod grip for large disks), the participant released the spacebar and pantomimed a grasp towards the on-screen disk. Pantomime grasps were defined as hand gestures whereby the hand approached the screen until the fingers contacted the contour of the disk, as they would do in an actual grasp. At the release of the spacebar, the target disappeared (i.e., the target disk offset, such that participants pantomimed the grasp relying on what they had seen during the motor preparation phase, without online visual feedback about the target), the PRT of the current trial was stored, and MATLAB issued a trigger to mark the target offset. Last, the participant brought back the hand to the starting position and waited for the appearance of the red cross indicating that the next trial could be started (the interval between the target disk offset and the red cross lasted 3 s, giving ample time to the participant to perform the movement). The experiment lasted about 1 h, plus approximately 30 min for setup including fitting the EEG cap.

2.8. EEG data acquisition and pre-processing

EEG data was recorded from 64 electrodes using an Active Two amplifier system (BioSemi, Amsterdam, Netherlands, http://www.biosemi.com). Electrodes were positioned according to the extended 10–20 system (Nuwer et al., 1998). To record the vertical (VEOG) and horizontal electrooculograms (HEOG), four additional leads were placed above and below the left eye and on the outer canthi of the left and right eyes. EEG from all channels was acquired concerning the common mode sense (CMS) electrode at a sampling rate of 512 Hz. Pre-processing procedures were run in MATLAB by means of the EEGLAB toolbox (Delorme and Makeig, 2004; version 14.1.2b) and custom scripts. First, the continuous EEG was split into epochs offline. Stimulus locked epochs began 100 ms prior to target onset and ended 1000 ms following target onset. Stimulus-locked ERPs were aligned to a 100 ms pre-onset onset baseline. Response-locked epochs began 1000 ms before the initiation of the response, and ended 200 ms after the movement onset, and were aligned to a 100 ms baseline from 1000 to 900 ms prior the movement onset. ERPs waveforms of each trial for each participant were digitally filtered (second-order zero-phase-lab band filter, 0.1–25 Hz), and the filtered individual ERPs waveforms were obtained averaging relevant trials for each condition. Then, EEG artifacts were removed using the SCADS procedure with standard parameters (Junghghöfer et al., 2000; Gruss and Keil, 2019; Harrison et al., 2015; Johnen and Harrison, 2019). This procedure detects individual channel artifacts and then transforms the data to average reference to detect global artifacts. Epochs that contained more than 10 unreliable electrodes were excluded from analysis based on of the distribution of their amplitude, standard deviation, and gradient. For the remaining epochs, data from artifact-contaminated electrodes was replaced by a statistically weighted spherical interpolation using the complete set of channels. Across all participants and all conditions, the procedure rejected approximately 30% of epochs as contaminated.

2.9. ERPs analysis

LRP's for right hand movements were measured by calculating the difference between potentials at the C3 and C4 channels (C3–C4; Smulders, Miller, and Luck, 2012). The target-locked P300 was scored at the Pz electrode. For the LRP and P300 components, we derived both amplitude and latency measures. To this aim we adopted different strategies depending on the type of ERP component. The LRP amplitude is known to reflect variations in the amount of inhibition involved in the response, with greater amplitudes reflecting a greater lack of inhibitory success (for instance, see DeJong et al., 1990). The LRP waveform usually consists of an early, quasi-zero trace followed by a later, monotonous negativity reaching the peak negative amplitude. There is some evidence that the temporal location of onsets and peaks in LRPs can vary depending on task manipulations (for instance, see Falkenstein et al., 1994). Thus, we computed amplitudes, onsets, and peaks by different methods to examine whether results were robust to changes in estimation approaches.

2.10. Estimation based on averaging from the raw data

In a first approach, we estimated amplitudes, onsets, and peaks directly from each participant's raw data. The LRP amplitude was then defined as the average μV value of the area under the curve within appropriate time windows both for pincer and pentapod grips, chosen by visual inspection of individual potentials. Temporal locations of LRP onsets and peaks were also detected within appropriate time windows based on visual inspection (see Results section for details). The LRP onset was defined as the millisecond at which the waveform reached the maximum (MAX) amplitude value; the peak, instead, was defined as the millisecond at which the waveform reached the minimum (MIN) amplitude value. The advantage of estimation based on the raw data is that no assumptions, modelling, or transformations are involved. Random fluctuations between participants can however affect the ability to reliably estimate the temporal locations of specific features such as onsets and peaks.

2.11. Estimation based on averaging, segmented regression, and jackknifing

In a second approach to the LRPs analysis, we applied a segmented regression procedure (Schwarzenau et al., 1998). In standard approaches, LRPs onsets are estimated detecting the time at which the amplitude exceeds an absolute or relative criterion (i.e., for instance, at −1 μV or at the 80% of the maximum amplitude, Ulrich and Miller, 2001). However, these strategies are arbitrary and do not work well in the presence of task-related differences in LRP waveforms. In contrast, fitting a segmented regression is less arbitrary in that the whole LRP waveform is used to estimate timings (Schwarzenau et al., 1998; Mordkoff and Gianaros, 2000). We defined the onset as the knot of the fitted segmented regression whereby the potential started to decrease and continued to decrease, and the peak as the knot where the potential reached the minimum amplitude value before turning back towards zero. The number of knots was chosen from visual inspections of grand average waveforms. Segmented regressions were fitted using the "segmented" package in R (Muggeo, 2008). To model individual differences, segmented regression was combined with a jackknife procedure (Miller et al., 1998; Ulrich and Miller, 2001; Miller et al., 2009). In the jackknife, *n* subsamples of LRP grand averages are computed by successively omitting from each subsample the LRP data of a different participant, *n* being the number of participants (in our case, 22). The LRP onset and peak latency were therefore estimated by fitting a segmented regression to each participant's jackknifed grand average. The whole procedure was applied both to the R-LRP and S-LRP data.

2.12. P300 analysis

For the P300 component we measured amplitude and peak latency. Grand average waveforms were computed by averaging individual potentials, then a spline smoother was applied. Amplitudes were defined as the average μV value of the area under the curve within an appropriate time window chosen by visual inspection of grand average waveforms. In contrast to LRPs, for P300 components we estimated peaks as the unique ms values at which the waveform reached its maximum (see Results section for details).

2.13. Statistical comparisons

Because ERP datasets are rich in random fluctuations, there is a relatively high risk of observing false positives (Luck and Gaspelin, 2017). This is especially true when making comparisons within many factors or performing several pairwise comparisons (Brandstätter, 1999; Steiger, 2004). Accordingly, we sought to avoid unnecessary comparisons and limited the analysis to our specific predictions (see also Brenner, 2016). To this aim, whenever appropriate we fitted multilevel linear mixed-effect models (LMM) using the *nlme* package in R (Pinheiro, Bates, DebRoy, Sarkar, and R Core Team, 2017). In comparison to traditional linear modelling, which uses ordinary least-squares, mixed-effects modelling uses maximum-likelihood estimation. This allowed us to predict participant-by-participant variation in model parameters (called random effects) and to discount these individual differences to compute within-participant confidence intervals around estimates of fixed effects, while avoiding drawbacks typically associated with traditional models, such as deficiencies in statistical power, individual differences in repeated measures designs, and unprincipled ways of dealing with heteroskedasticity and non-spherical error variance (see Baayen et al., 2008). In addition, but not less important, mixed-effects modelling allowed us to dispose of null-hypothesis testing, in accord with current recommendations on analytical approaches in psychology and behavioural neuroscience (see Cumming, 2014; Kline, 2004). Thus, for all dependent measures (PRT, LRP, and P300), we compared incongruent conditions with their corresponding (congruent) baselines by constructing appropriate confidence intervals (CIs) around estimates of central tendency. For estimates derived from jackknifing, which compare variation in the quantity of interest across subsets of the total sample instead of across individuals, CIs around the within-participant incongruent vs congruent means were instead computed using the jackknife standard error formula recommended by Miller et al. (1998). R scripts for modelling all data are available in the Open Analysis document (https://osf.io/yvsg5/).

3. Results

Plots of the individual ERP waveforms and tables resuming the main results are viewable in the Open Supplemental Material document (https://osf.io/yvsg5/).

3.1. Preview reaction times

3.1.1. Data validation

PRTs were defined as the duration of the discretional temporal window between the onset and offset of the target disk (i.e., the press and release of the spacebar, respectively). Firstly, we checked the PRT distribution for the presence of anomalous values. A cut-off of ≤150 ms was deemed appropriate to identify anticipatory responses. Based on this criterion, a total of 57 PTRs were removed. Then, abnormally long PRTs were identified as those exceeding the following criterion for robust outlier detection (Leys et al., 2013):

$$\text{abs}(\text{PRT} - \text{MED}) / \text{MAD} > 3$$

where *abs* refers to absolute value, PRT is a vector of preview reaction times, MED is the median of this vector, and MAD is its median absolute deviation. A total of 199 trials exceeded this criterion. Together with trials identified as anticipatory responses, a total of 256 datapoints were discarded (4.85% of the whole PRTs dataset). Thus, all statistics used in further analyses were computed on the validated dataset.

3.1.2. Normalization of the PRT distribution

Fig. 3 (upper panel, left) shows the PRT distribution. As is typical for response times, this distribution was markedly asymmetrical (skewness = 1.88) and unbalanced in relation to the relative frequency of cases in the center and in the tails (kurtosis = 6.91). We applied a Box-Cox procedure (Box and Cox, 1964; Osborne,

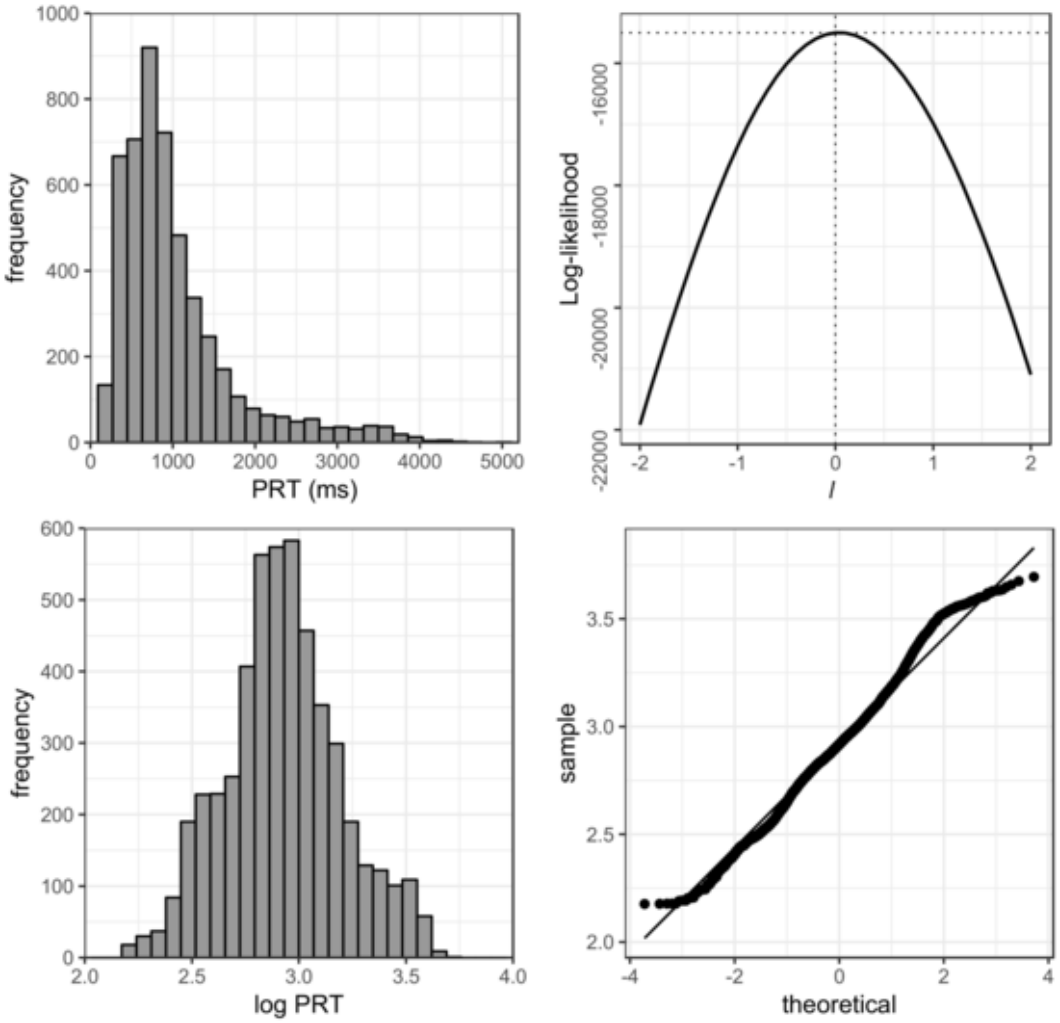

Fig. 3. Distribution of preview reaction times before and after the logarithmic transformation. Upper row left: raw times; upper row right: Box-Cox likelihood plot suggesting that the best transformation is the log. Lower row left: log-transformed times; lower row right: plot of sample quantiles against theoretical quantiles in a normal distribution.

2010) to identify the best transformation for normalizing the raw data (Fig. 3, upper panel, right plot). This indicated that a logarithmic transformation made the PRT distribution reasonably similar to a normal distribution (skewness = 0.13; kurtosis = 2.94; Norm = 0, 3), as shown in Fig. 3 (lower panel, left and right plots). Accordingly, the analysis was performed on the log-transformed data. For ease of interpretation, however, estimated effects will be reported after an inverse anti-logarithmic transformation as geometric means expressed in milliseconds. Thus, each participant had four geometric means (i.e., one for each of the four distractor-target pairs). CIs around estimates that are symmetrical above and below arithmetic mean on the log-scale become asymmetrical after the inverse transformation, but retain their usual interpretation.

3.1.3. Within-participant structure of the data

Fig. 4 presents individual averages of the log-PRTs in the paired incongruent and congruent conditions, separately for the pincer and pentapod grips. The diagonal line is the locus of no within-participant difference. These plots show that the majority of participants had higher mean PRTs in both incongruent conditions, but this trend was much stronger when the test required a pincer grip. In the congruent conditions, the geometric mean of PRTs were 788 and 841 ms when participants prepared pincer and pentapod grips, respectively. In the incongruent conditions, they were 848 and 864 ms for pincer and pentapod grips, respectively. Thus, overall PRT were higher in the incongruent conditions than the congruent, and when responding with pentapod than pincer grips.

3.1.4. PRTs modelling

Standard errors for CIs were based the LMM, with condition (i.e., each distractor - target pair) as the fixed-effects factor and participants as random-effects. For model comparisons we performed likelihood ratio tests using Chi-Square (χ^2), following Winter (2013). Model selection was performed as follows. First, we compared the fit of a generalized least squared (GLS) null model with fixed intercept (model 1) with a null model with random intercept (model 2) using a maximum likelihood criterion. Model 2 outclassed model 1, (AIC (1) = 0.21, AIC (2) = −210.2; likelihood ratio (1 vs 2): $\chi^2(3) = 212.83$, $p < 0.0001$), confirming non-negligible interindividual variability in PRTs. Next, we generated model 3 by adding the experimental condition (as a fixed effect) to model 2. The comparison between model 2 and model 3 revealed that the latter provided an even better fit (AIC (6) = −220.68; likelihood ratio (2 vs 3): $\chi^2(6) = 16.06$, $p = 0.001$). That is, comparing model 3 to model 2 supported the conclusion that PRT's varied not only between participants but were also modulated by the type of distractor - target pair (congruent or incongruent). The insets of Fig. 4 present LMM estimates of such fixed effects and their 95% CIs. Comparisons can be

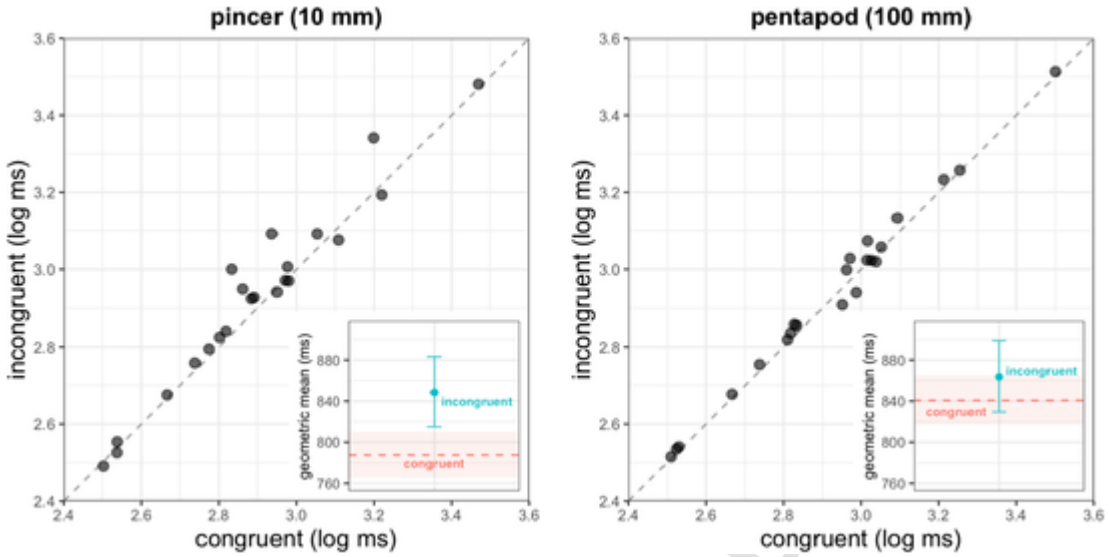

Fig. 4. Main plots: Within-participant structure of the PRT data. Each datapoint represents the arithmetic average of pincer or pentapod log-PRTs of one participant, in the paired congruent and incongruent conditions. The diagonal line represents the no within-participant difference (average congruent = average incongruent). Insets: LMM-based 95% CIs around estimates of central tendency (geometric means) in the incongruent conditions (blue disks with error bars), plotted against the equivalent estimates for the baseline (congruent, red) conditions. (For interpretation of the references to color in this figure legend, the reader is referred to the web version of this article.)

performed by evaluating whether CIs of the effects cover their corresponding baseline.

3.2. Response-locked lateralized readiness potentials (R-LRPs)

Given that we predicted an effect on response-related LRP, we start by presenting the findings of the R-LRPs analysis. Next, we present results of the S-LRP. We conclude with the analysis of the P300 component.

3.2.1. Grand average waveforms

Fig. 5 presents R-LRP grand average waveforms (thick curves) obtained by averaging the individual potentials and applying a smoother. Grand averages exhibited a slow negative trend over time, confirming that motor preparation occurred prior to response onset. For pincer grips (left plot), the two waveforms had approximately the same amplitude and time course from −1000 to −200 ms; then, the R-LRP of the test condition peaked later and the amplitude reduced, compared to the baseline condition. For pentapod grips (right plot), instead, the R-LRP of the congruent condition became negative around −600 ms, whereas the R-LRP of the incongruent condition became negative later around −400 ms; in contrast, both conditions appeared to peak around −150 ms. Finally, the amplitude of the test condition reduced in comparison to the baseline condition.

3.2.2. Estimation of amplitudes

For each participant's RLRP dataset, amplitudes were calculated as the mean value of the area under the curve within a −400 to 0 ms time window, both for pincer and pentapod grips. We compared incongruent conditions to the relevant congruent condition for each grip. Thus, each participant had a paired incongruent-congruent am-

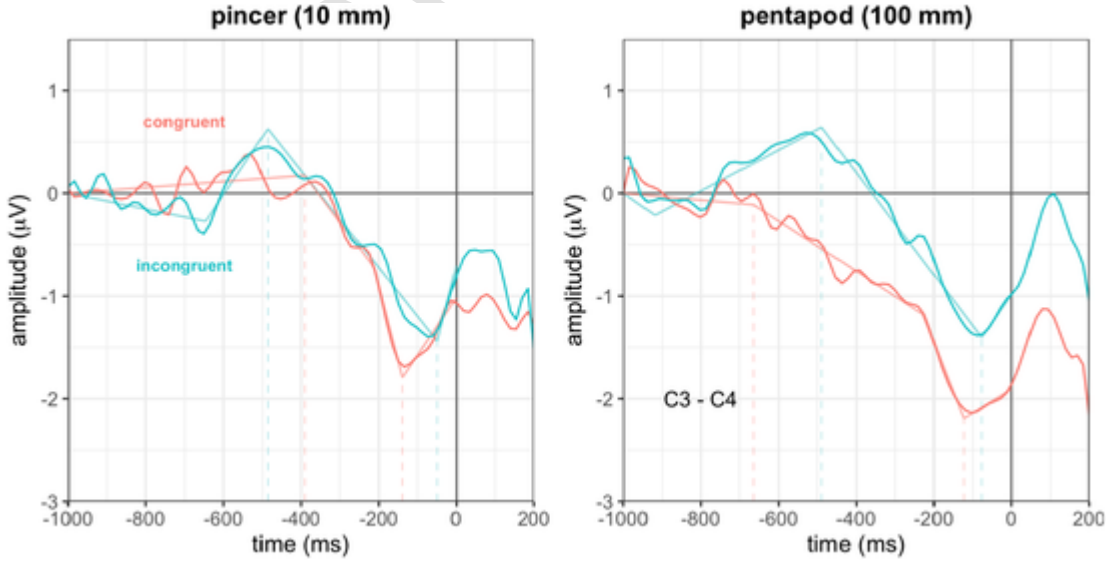

Fig. 5. R-LRP grand average waveforms (thick curves) and average jackknifed segmented regressions (thin lines) as a function of grip (pincer, left panel; pentapod, right panel) and congruence (congruent, red; incongruent, blue). Dashed vertical lines: average value of the onset and peak amplitude latency estimates of subsamples. Vertical black line: response onset. (For interpretation of the references to color in this figure legend, the reader is referred to the web version of this article.)

plitude estimate for both pincer and pentapod grip (22 estimates for each distribution).

3.2.3. Amplitude modelling

Statistical differences were evaluated comparing CIs based on the LMM, with conditions as the fixed-effects factor and participants as random-effects. We compared model 1 with model 2 (i.e., fixed intercept vs random intercept), then model 2 with model 3 (i.e., adding the experimental condition as fixed effect). Model 2 outclassed model 1, (AIC (1) = 421.91, AIC (2) = 392.44; likelihood ratio (1 vs 2): $\chi^2(2) = 31.37$, $p < 0.0001$), confirming non-negligible interindividual variability in amplitude. However, the comparison between model 2 and model 3 revealed that this latter did not provide a better fit (AIC (3) = 395.02; likelihood ratio (2 vs 3): $\chi^2(3) = 3.4$, $p = 0.33$). Thus, although amplitudes were affected by individual differences, the distractor-target pair did not introduce modulations. For pincer grips, means and CIs were: −0.83 ± −0.65 μV for the baseline (congruent) condition, and −0.64 ± −0.91 μV for the test (incongruent) condition; for pentapod grips, means and 95% CIs were: −1.47 ± −0.65 μV for the congruent condition, and −0.83 ± 0.91 μV for the incongruent condition.

3.2.4. Estimation of latencies of onsets and peaks

We sought to determine whether onsets and peak amplitude latencies of incongruent conditions were different from their relevant baseline. For each participant's R-LRP waveform, onsets were extracted within a −600 to −200 ms time window for pincer grips, and within a −800 to −450 ms time window for pentapod grips. Peak latencies, instead, were extracted within a −150 to −50 ms time window for both grips. Thus, each participant had four paired incongruent-congruent latency estimates, yielding four distributions each of 22 estimates (i.e., pincer onset, pincer peak latency, pentapod onset, and pentapod peak latency).

3.2.5. Within-participant structure of onsets and peaks

The within-participant structure of onset and peak latencies is presented in Fig. 6, main plots. These plots display two main features. First, the between-participant variability in the timing of onsets (left column) is much larger than the variability in the timing of peaks (right column). Second, and most important for our current purpose, individual datapoints are about equally located above and below the no-difference locus (diagonal line) of pincer onsets (upper left panel), whereas they cluster above it in pentapod onsets (lower left). Conversely, individual datapoints cluster above the diagonal for pincer peaks (upper right), but not for pentapod peaks (lower right). Thus, the graphical inspection of within-participant differences suggested that R-LRPs onset was delayed in the test condition, relative to the baseline, for pentapod but not for pincer grips. In contrast, the peak of the waveform seemed to occur later for pincer grips than for pentapod.

3.2.6. Latencies modelling

As in the previous analysis, we used LMM to calculate CIs. The same model was applied to onset and peak estimates. For onsets, the null model 1 (fixed intercept) was compared with the null model 2 (random intercept). Model 2 did not provide a better fit than model 1, (AIC(1) = 1120.68, AIC(2) = 1122.683, likelihood ratio (1 vs 2): $\chi^2(3) = 0.00$, $p = 0.99$). Then, model 3 was generated by adding the experimental condition (as a fixed effect) to model 2. Model 3 clearly yielded a better fit compared to model 2 (AIC(3) = 1080.091; likelihood ratio (2 vs 3): $\chi^2(6) = 48.58$, $p < 0.001$). For peak latencies, the comparison between model 1 and 2 provided weak support for a difference (AIC(1) = 867.14, AIC(2) = 865.54, likelihood ratio (1 vs 2): $\chi^2(3) = 3.57$ $p = 0.058$). The comparison between model 2 and model 3 again revealed the superiority of model 3, (AIC(3) = 862.95, likelihood ratio (2 vs 3): $\chi^2(6) = 8.6$, $p < 0.05$). Thus, both onsets and peaks were not modulated by interindividual variability but were modulated by the experimental condition.

3.2.7. Segmented regressions on jackknifed subsamples

We performed a second analysis applying the segmented regression method combined with a jackknife procedure (see Methods section for details). First, we computed the 22 R-LRP jackknifed subsamples. Then, we fitted the regressions segmented into three knot-points to best capture the fit of jackknifed subsamples. Superimposed on waveforms, Fig. 5 presents average segmented regression fitted on jackknifed participants (shaded lines) as a function of grip and congruence. The average fit was obtained by averaging the individual parameters of each participant's jackknifed fit for each condition. The knots marked by vertical dashed lines represent the average R-LRP onset and peak latency. At least from a visual inspection, the segmented regressions show the same asymmetric pattern seen in the previous analysis.

3.2.8. Estimation of amplitudes

Given that jackknifed subsamples produce estimates that are less affected by random fluctuations, we extended the time window for calculating the average amplitude (from −600 to 0 ms for both grips). As in the raw data analysis, test conditions were compared with the relevant baseline condition for each grip. Thus, each participant had a paired incongruent-congruent mean amplitude value for both pincer and pentapod grips (22 estimates for each distribution).

3.2.9. Amplitudes modelling

Statistical differences were evaluated computing CIs around the mean values of each within-participants distribution. In each comparison, we computed the difference of test minus baseline estimates, then we calculated the standard error of these distributions. Note that in this case standard errors were computed with the formula for jackknifed subsamples (Miller et al., 1998). Resulting means and CIs (95%) were: 0.18 ± 0.64 μV for the incongruent-minus-congruent pincer distribution; 0.86 ± 0.60 μV for the incongruent-minus-congruent pentapod distribution. In contrast with the amplitude analysis on the raw data, these results revealed that the amplitude in the incongruent condition reduced relative to baseline for pentapod targets after pincer distractors, but not for pincer targets after pentapod distractors or between the two baselines.

3.2.10. Estimation of latencies of onsets and peaks

In each jackknifed subsample the onset and the peak latency were identified as the millisecond corresponding to the knot estimated by the segmented regression. Thus, each jackknifed participant had the same four paired incongruent-congruent latency estimates, yielding four distributions of 22 estimates.

3.2.11. Latencies modelling

In each comparison we calculated incongruent minus congruent differences and then computed the relative standard errors for jackknifed subsamples. CIs were computed around the averages of these incongruent-minus-congruent within-participant distributions. Fig. 6 right insets present these CIs for the R-LRP jackknifed latency differences. Comparisons can be directly made by evaluating whether the CIs cover zero. R-LRPs of pincer grips in the incongruent condition peaked later compared to baseline, confirming what we found in the raw data analysis. In contrast, for pentapod grips both onset and peak latency estimates in the incongruent condition were different from baseline. While the two analysis we conducted revealed a con-

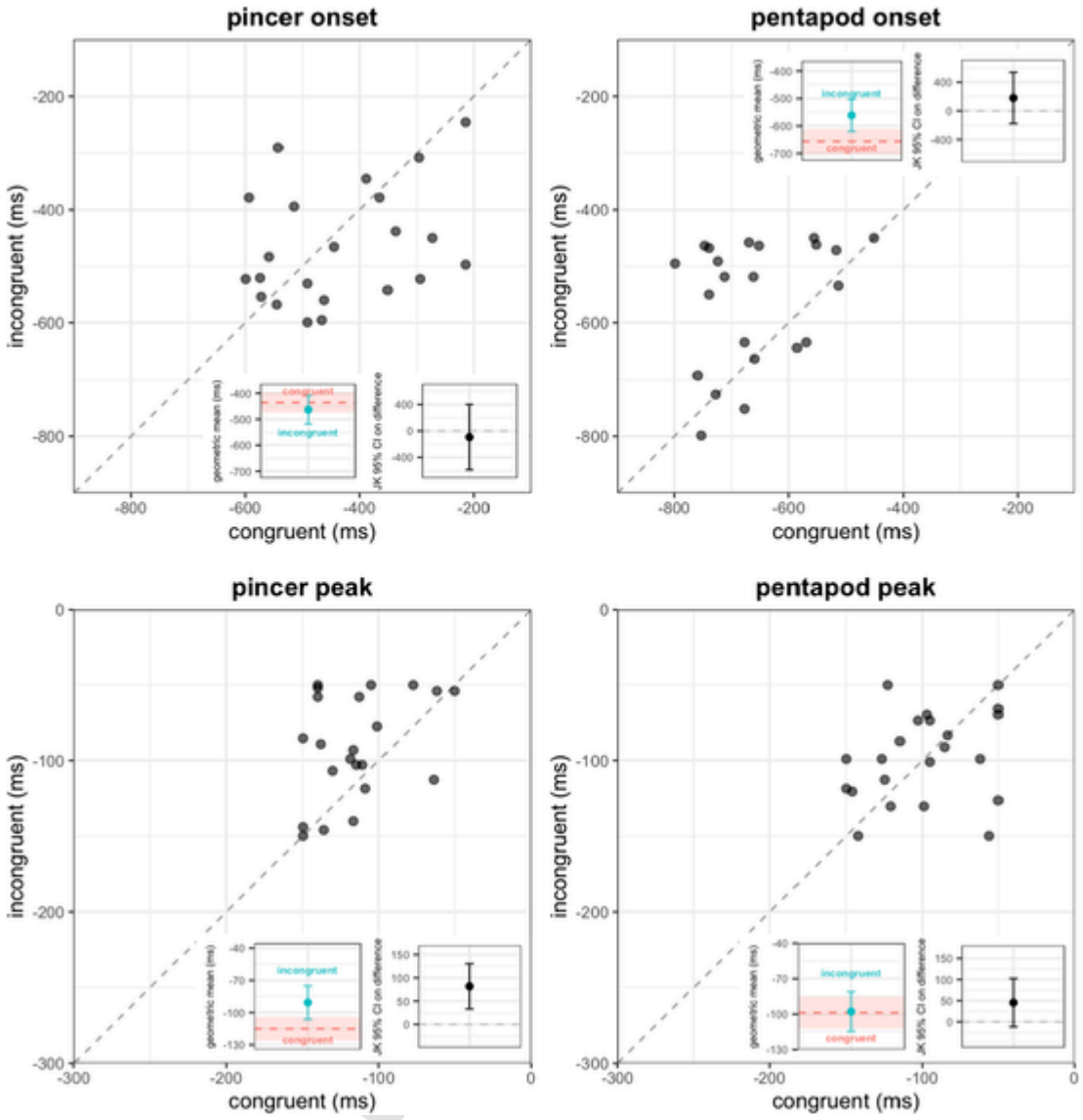

Fig. 6. Main plots: within-participant structure of the R-LRP data. Each datapoint represents the estimated pincer or pentapod latencies for the onset or the peak of the waveform, in one participant, in the paired congruent and incongruent conditions. The diagonal line represents the no within-participant difference (average congruent = average incongruent). Left insets: LMM-based 95% CIs around estimates of central tendency (geometric means) in the incongruent conditions (blue disks with error bars), plotted against the equivalent estimates for the baseline (congruent, red) conditions. Right insets: Jackknife-based CIs on the mean congruent vs incongruent difference. (For interpretation of the references to color in this figure legend, the reader is referred to the web version of this article.)

sistent pattern for pincer grips, for pentapod grips they do not fully agree suggesting more uncertainty on whether incongruent distractors affected the onset of the waveform.

3.3. Stimulus-locked lateralized readiness potentials (S-LRPs)

The two analyses presented above revealed that incongruent distractors delayed the time course of R-LRP waveforms. Thus, this finding supports the idea that the motor system required a cost of updating the first, implicit grip to the second, explicit grip. Nevertheless, we could not exclude that a similar effect influenced the motor program also during an earlier stage of the sensorimotor evaluation of the target disk. Thus, we inspected the LRP potentials as a function of the target disk onset.

3.3.1. Grand average waveform

Fig. 7 presents S-LRP grand average waveforms (thick curves) as a function of grip and congruence, obtained by averaging the individual potentials and applying a smoother for a better visualisation. Based on visual inspection of grand averages, there are no differences between the two conditions either for pincer or pentapod grips. Indeed, the onset, which is identifiable at about 100–200 ms, appeared to be almost identical between conditions for both grips. The same is true for the peak latency which is identifiable at about 400 ms. Besides, amplitudes show a large degree of overlap. The absence of any difference is also clear from the average segmented regressions showed in Fig. 7 (thin lines). Thus, we ruled it unnecessary to run statistical comparisons.

3.4. P300 component

As a last step, we analyzed the P300 component to verify whether earlier attentional processes delayed the motor preparation.

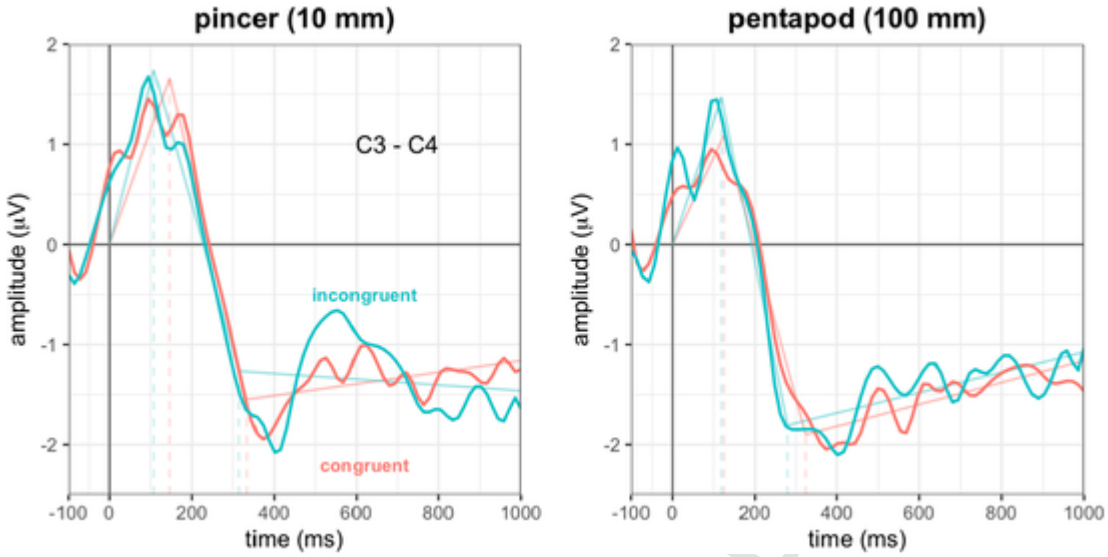

Fig. 7. S-LRP grand average waveforms (thick curves) and average segmented jackknifed regressions (thin lines) as a function of grip (pincer, left panel; pentapod, right panel) and congruence (congruent, red; incongruent, blue). Dashed vertical lines: average value of the onset and peak amplitude latency estimates of subsamples. Vertical black line: stimulus onset. (For interpretation of the references to color in this figure legend, the reader is referred to the web version of this article.)

3.4.1. Grand average waveform

Fig. 8 presents grand averaged P300 components as a function of grip and congruence. At least qualitatively, the figure suggests that the amplitude in the incongruent conditions was higher compared to congruent conditions whereas waveforms clearly peaked at the same time. Thus, we ruled it unnecessary to run statistical test on peak latencies and compared amplitudes only.

3.4.2. Estimation of amplitudes

Amplitudes were calculated as the mean value of the area under the curve within a 250 ms to 500 ms time window for each condition and each participant. Thus, each participant had two paired incongruent-congruent amplitude estimates for each grip (22 datapoints in each distribution).

3.4.3. Amplitude modelling

Statistical differences were evaluated with CIs calculated from a LMM. Model 2 (random intercept) outclassed model 1 (fixed intercept) revealing a better fit (AIC (1) = 381.48, AIC (2) = 341.40, likelihood ratio (1 vs 2): $\chi^2(3) = 42.07$ $p < 0.001$). Model 3 (by adding the experimental condition) outclassed model 2 and revealing an even better fit (AIC (3) = 325.89, likelihood ratio (2 vs 3): $\chi^2(6) = 21.49$, $p = 0.0004$). Thus, both interindividual variability and the experimental condition introduced non-negligible modulations in amplitude. Fig. 9 presents the CIs around the means calculated in the model: comparisons can be performed directly by evaluating whether CIs of incongruent conditions cover the relevant baseline. The S-LRP and P300 analyses indicated that no reliable delays occurred due to earlier attentional or sensory processes related to the target disk. These results strengthen our interpretation that PRT costs are due to an update of motor preparation.

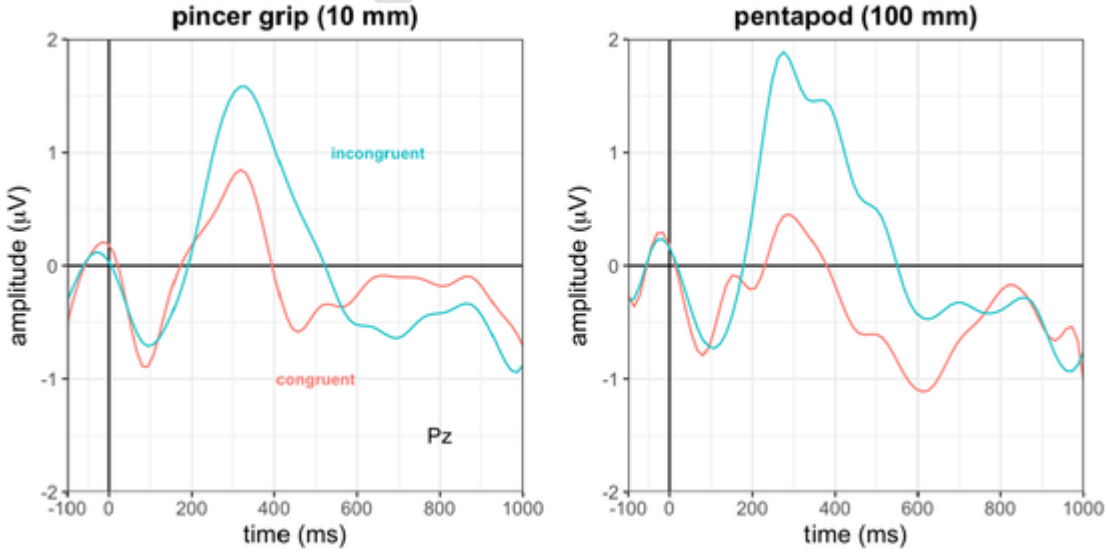

Fig. 8. P300 component grand averages as a function of grip (left, pincer; right, pentapod) and congruence (red, congruent; blue, incongruent). Vertical black line: stimulus disk onset. (For interpretation of the references to color in this figure legend, the reader is referred to the web version of this article.)

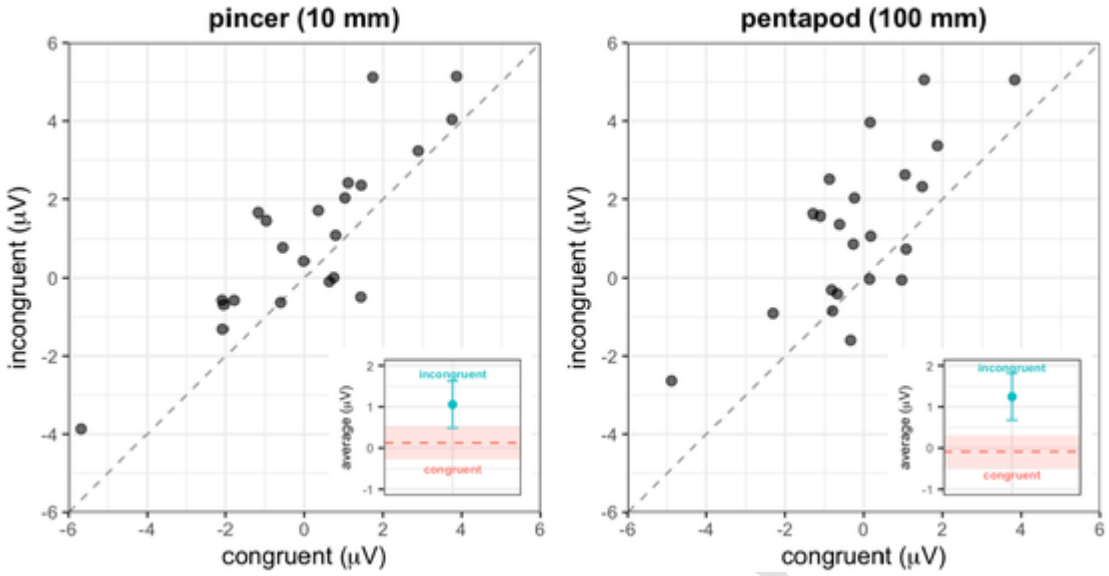

Fig. 9. Main plots: Within-participant structure of the P300 data. Each datapoint represents the estimate of pincer or pentapod amplitude of one participant, in the paired congruent and incongruent conditions. The diagonal line represents the no within-participant difference (average congruent = average incongruent). Insets: LMM-based 95% CIs around estimates of central tendency (average) in the incongruent conditions (blue disks with error bars), plotted against the equivalent estimates for the baseline (congruent, red) conditions. (For interpretation of the references to color in this figure legend, the reader is referred to the web version of this article.)

4. Discussion and conclusion

According to the TVSH, vision-for-action continuously updates visual information to support the control of actions in real time. This implies that visuomotor codes elicited before an action (i.e., the temporal context) should be rapidly overwritten by codes relevant to the current motor response. For instance, representations elicited by viewing a distractor object would not modify motor preparation parameters (i.e., in our case, the PRT) for grasping a successive target object. To test this prediction, we analyzed PRTs, LRPs, and the P300 component during a pantomimed grasping movement directed to a target disk preceded by a different distractor disk. Our results provide, for the first time, consistent behavioural and electrophysiological evidence that previous implicit visuomotor processes interact with motor preparation for a successive actual action on a different object. Key implications of our findings are discussed below.

4.1. The effect of distractors on PRTs is asymmetric

The time participants spent observing the target and preparing the response depended on the size of the previous distractor disk. When distractors and targets were different in size, PRTs were longer overall, but there was a notable difference between trials calling for pincer vs pentapod grips. After a large distractor, PRTs associated to pincer grips involved a large cost (i.e., the PRT was considerably longer). After a small distractor, in contrast, PRTs associated to pentapod grips involved only a relatively small cost with weak statistical support for a difference with the baseline. These results are very similar to those of Pisu et al. (2020) and support the notion that seeing the distractor affected the preparation of the response for the test. This distractor effect, however, appears to be qualitatively different from classical visuomotor priming in that the observed cost for incongruent distractor-test pairs (which is predicted by visuomotor priming) is much larger for small disks after large distractors than for large disks after small distractors. The effect of distractors on PRT's is therefore asymmetric, unlike standard visuomotor priming which predicts a symmetric effect of congruency. After considering several possible accounts of their results, including visuomotor priming and finger-based facilitation, Pisu et al. (2020) proposed that their results may be due to asymmetric generalization of precision when setting motor parameters in an action's planning phase. The current results are consistent with this possibility.

4.2. R-LRPs also revealed an asymmetric effect, but S-LRPs and P300 components did not

We sought to determine if PRT costs corresponded to differences in LRPs, which are ERP signatures of movement preparation. Based on asymmetric generalization of precision, one would expect a delay in some component of the R-LRP waveform when preparing a pincer grip after a large distractor, but a negligible or at least weaker delay in the opposite condition. Our results indicate that one such delay is measurable for the negative peak in the late part of the waveform. Specifically, when responding with pincer grips, the peak amplitude of the R-LRP waveform occurred later after an incongruent (i.e., large) distractor than it did after a congruent (i.e., small) distractor. When responding with pentapod grips, conversely, the peak amplitude occurred at about the same time with both distractors. In contrast, when using pentapod grips the onset was delayed after the presentation of a smaller distractor disk, whereas the peak latency was relatively unaffected. Moreover, in contrast S-LRPs did not show differences between congruent and incongruent conditions and both grips. This suggests that early perceptual processing evaluation of the target features was not affected by the pre-activated motor program. Furthermore, the analysis of the P300 components revealed higher average amplitudes in incongruent conditions than congruent. This is consistent with the idea that updating visual information recruited additional attentional resources. However, P300 components peaked at the same time in both conditions and both grips. Hence, the contextual updating associated to incongruent distractor - target pairs did not further modulate attentional processes. Taken together, these results confirm that implicit processing related to the distractor presentation did have an effect on the preparation of the pantomimed grasp for the test object and, at least under these conditions, this effect was most likely due to motor rather than sensory or attentional processes.

4.3. Caveats and limitations

One important difference between the protocol employed in the current study and that of Pisu et al. (2020) is that in their case participants performed an actual grasp directed to a solid three-dimensional disk and picked it up at the end of the response. Here, instead, participants performed a pantomimed grasp towards a disk that was drawn on a computer screen. Although they moved the hand towards the screen rather naturally, in the final part of the grasp they could not pick up the disk as in Pisu's study. The impact of these differences on the interpretation of the current result is, at present, not completely clear. Goodale et al. (1994) and Westwood et al. (2000) suggested that pantomimed actions involve interactions of ventral stream processes with dorsal visuomotor processes, while actual object-directed actions depend solely on dorsal circuits. However, an fMRI study showed that pantomimed grasps can recruit dorsal neural circuits, as do real grasps (see Króliczak et al., 2007). Whether this is true for all pantomimes and for all phases of an action is also presently not clear. In our study, we focused on motor preparatory processes, and one feature of our data suggests that the pictorial nature of our 2D stimuli might have affected motor preparation. In the congruent conditions, PRTs were longer for pentapod than for pincer grips (compare the pink bands in Fig. 4). This is the opposite of what was observed by Pisu and collaborators, and of what one would expect based on the precision which is presumably required in a motor program aimed at a large vs a small object. The latter should require a more precise program, which in turn might be expected to imply longer preparatory processing. We are currently designing further studies aimed at testing possible differences between preparation and execution of pantomimed or real pincer and pentapod grasps. As suggested by an anonymous reviewer, this could be done by combining the EEG with augmented reality to create a virtual 3D object or, in alternative, with a procedure for displaying actual three-dimensional objects. We stress however that, even if the current effect did involve a contribution from the ventral system, this would weaken its implications for the dorsal amnesia hypothesis (see Introduction), but would not undermine our conclusion that the mere sight of the (irrelevant) distractor modulated R-LRPs during motor preparation. This finding provides useful insights into the nature of potential temporal interactions within cortical networks for motor planning (Castiello, 2005; Schenk et al., 2011; De Sanctis et al., 2013; Budisavljevic et al., 2018).

Funding

This research did not receive any specific grant from funding agencies in the public, commercial, or not-for-profit sectors.

CRediT authorship contribution statement

Stefano Uccelli: Conceptualization, Data curation, Formal analysis, Investigation, Methodology, Software, Project administration, Visualization, Writing - original draft, Writing - review & editing. **Letizia Palumbo:** Investigation, Writing - review & editing, Supervision. **Neil Harrison:** Investigation, Software, Writing - review & editing, Supervision. **Nicola Bruno:** Conceptualization, Formal analysis, Methodology, Project administration, Visualization, Writing - review & editing, Supervision.

Declaration of competing interest

None.

Appendix A. Supplementary data

Supplementary data to this article can be found online at https://doi.org/10.1016/j.ijpsycho.2020.10.007.

References

Anderson, S.J., Yamagishi, N., Karavia, V., 2002. Attentional processes link perception and action. Proc. R. Soc. Lond. Ser. B 269, 1225–1232.
Baayen, R.H., Davidson, D.J., Bates, D.M., 2008. Mixed-effects modeling with crossed random effects for subjects and items. J. Mem. Lang. 59 (4), 390–412.
Box, G.E.P., Cox, D.R., 1964. An analysis of transformations. J. R. Stat. Soc. 26 (2), 211–252.
Brainard, D.H., 1997. The psychophysics toolbox. Spatial Visions 10, 433–436.
Brandstätter, E., 1999. Confidence intervals as an alternative to significance testing. Methods Psychol. Res. 4 (2), 33–46.
Brenner, E., 2016. Guest editorial: why we need to do fewer statistical tests. Perception 45 (5), 489–491.
Bruno, N., Garofalo, G., Daneyko, O., Riggio, L., 2018. Visual similarity modulates visual size contrast. Acta Psychol. 188, 122–130.
Buccino, G., Sato, M., Cattaneo, L., Riggio, L., 2009. Broken affordances, broken objects: a TMS study. Neuropsychologia 47, 3074–3078.
Budisavljevic, S., Dell'Acqua, F., Castiello, U., 2018. Cross-talk connections underlying dorsal and ventral stream integration during hand actions. Cortex 103, 224–239.
Cant, J.S., Westwood, D.A., Valyear, K.F., Goodale, M.A., 2005. No evidence for visuomotor priming in a visually guided action task. Neuropsychologia 43 (2), 216–226.
Castiello, U., 2005. The neuroscience of grasping. Nat. Rev. Neurosci. 6, 726–736.
Chao, L.L., Martin, A., 2000. Representation of manipulable man-made objects in the dorsal stream. NeuroImage 12 (4), 478–484.
Chong, I., Proctor, R.W., 2020. On the evolution of a radical concept: affordances according to Gibson and their subsequent use and development. Perspect. Psychol. Sci. 15 (1), 117–132. https://doi.org/10.1177/1745691619868207.
Craighero, L., Fadiga, L., Umiltà, C., Rizzolatti, G., 1996. Evidence for visuomotor priming effect. NeuroReport 8, 347–349.
Craighero, L., Fadiga, L., Rizzolatti, G., Umiltà, C., 1998. Visuomotor priming. Vis. Cogn. 5, 109–125.
Cumming, G., 2014. The new statistics: why and how. Psychol. Sci. 25 (1), 7–29.
De Sanctis, T., Tarantino, V., Straulino, E., Begliomini, C., Castiello, U., 2013. Co-registering kinematics and evoked related potentials during visually guided reach-to-grasp movements. PLoS One 8, e65508. doi:10.1371/journal.pone.0065508.
DeJong, R., Coles, M.G.H., Logan, G.D., Gratton, G., 1990. In search of the point of no return: the control of response processes. J. Exp. Psychol. Hum. Percept. Perform. 16, 164–182.
Delorme, A., Makeig, S., 2004. EEGLAB: an open source toolbox for analysis of single-trial EEG dynamics including independent component analysis. J. Neurosci. Methods 134, 9–21. doi:10.1016/j. jneumeth.2003.10.009.
Donchin, E., Coles, M.G.H., 1988. Is the P300 component a manifestation of context updating? Behav. Brain Sci. 11, 357–374.
Eimer, M., 1998. The lateralized readiness potential as an on-line measure of central response activation processes. Behav. Res. Methods Instrum. Comput. 30, 146–156. https://doi.org/10.3758/BF03209424.
Falkenstein, M., Hohnsbein, J., Hoormann, J., 1994. Effects of choice complexity on different subcomponents of the late positive complex of the event-related potential. Electroencephalogr. Clin. Neurophysiol. 92, 148–160.
Feix, T., Romero, J., Schmiedmayer, H.B., Dollar, A.M., Kragic, D., 2015. The GRASP taxonomy of human grasp types. IEEE Trans. Human-Machine Syst. 46 (1), 66–77.
Gibson, J., 1979. The Ecological Approach to Visual Perception. Houghton Mifflin, Boston.
Goodale, M.A., Milner, A.D., 1992. Separate visual pathways for perception and action. Trends Neurosci. 15 (1), 20–25.
Goodale, M.A., Jakobson, L.S., Keillor, J.M., 1994. Differences in the visual control of pantomimed and natural grasping movements. Neuropsychologia 32, 1159–1178.
Gratton, G., Coles, M.G., Sirevaag, E.J., Eriksen, C.W., Donchin, E., 1988. Pre- and poststimulus activation of response channels: a psychophysiological analysis. J. Exp. Psychol. Hum. Percept. Perform. 14 (3), 331–344.
Green, P., MacLeod, C.J., 2016. SIMR: an R package for power analysis of generalized linear mixed models by simulation. Methods Ecol. Evol. 7 (4), 493–498. doi:10.1111/2041-210X.12504.
Grèzes, J., Decety, J., 2002. Does visual perception of object afford action? Evidence from a neuroimaging study. Neuropsychologia 40 (2), 212–222.
Grèzes, J., Tucker, M., Armony, J., Ellis, R., Passingham, E.E., 2003. Objects automatically potentiate action: an fMRI study of implicit processing. Eur. J. Neurosci. 17, 2735–2740.
Gruss, L.F., Keil, A., 2019. Sympathetic responding to unconditioned stimuli predicts subsequent threat expectancy, orienting, and visuocortical bias in human aversive Pavlovian conditioning. Biol. Psychol. 140, 64–74.
Harrison, N.R., Witheridge, S., Makin, A.D., Pegna, A.J., Wuerger, S.M., Meyer, G.F., 2015. The effects of stereo disparity on the behavioural and electrophysiological correlates of perception of audio-visual motion in depth. Neuropsychologia 78, 51–62.

Hesse, C., de Grave, D.D.J., Franz, V.H., Brenner, E., Smeets, J.B.J., 2008. Planning movements well in advance. Cognit. Neuropsychol. 25 (7–8), 985–995.
Jeannerod, M., 1981. Intersegmental coordination during reaching at natural visual objects. In: Long, J., Baddeley, A. (Eds.), Attention and Performance IX. Erlbaum, Hillsdale, NJ, pp. 153–168.
Jeannerod, M., Arbib, M.A., Rizzolatti, G., Sakata, H., 1995. Grasping objects: the cortical mechanisms of visuomotor transformation. Trends Neurosci. 18, 314–320.
Johnen, A.-K., Harrison, N., 2019. The effects of valid and invalid expectations about stimulus valence on behavioural and neural responses to emotional pictures. Int. J. Psychophysiol. 144, 47–55.
Junghghöfer, M., Elbert, T., Tucker, D.M., Rockstroh, B., 2000. Statistical control of artifacts in dense array EEG/MEG studies. Psychophysiology 37, 523–532. doi:10.1111/1469-8986.3740523.
Kappers, A.M.L., Bergmann-Tiest, W.M., 2014. Influence of shape on the haptic size aftereffect. PLoS One 9, 1–8.
Kline, R.B., 2004. Beyond significance testing: Reforming data analysis methods in behavioral research. American Psychological Association, Washington, DC.
Króliczak, G., Cavina-Pratesi, C., Goodman, D.A., Culham, J.C., 2007. What does the brain do when you fake it? An fMRI study of pantomimed and real grasping. J. Neurophysiol. 97 (3), 2410–2422.
Leuthold, H., Sommer, W., Ulrich, R., 1996. Partial advance information and response preparation: inferences from the lateralized readiness potential. J. Exp. Psychol. Gen. 125, 307–323.
Leys, C., Ley, C., Klein, O., Bernard, P., Licata, L., 2013. Detecting outliers: do not use standard deviation around the mean, use absolute deviation around the median. J. Exp. Soc. Psychol. 49 (4), 764–766.
Luck, S.J., Gaspelin, N., 2017. How to get statistically significant effects in any ERP experiment (and why you shouldn't). Psychophysiology 54, 146–157.
Magliero, A., Bashore, T., Coles, M., Donchin, E., 1984. On the dependence of P300 latency on stimulus evaluation processes. Psychophysiology 21, 171–186.
Maranesi, M., Bonini, L., Fogassi, L., 2014. Cortical processing of object affordances for self and others' action. Front. Psychol. 5 (538). doi:10.3389/fpsyg.2014.00538.
Marteniuk, R.G., Leavitt, C.L., MacKenzie, C.L., Athenes, S., 1990. Functional relationship between grasp and transport components in a prehension task. Hum. Mov. Sci. 9, 149–176.
Miller, J., Patterson, T., Ulrich, R., 1998. Jackknife-based method for measuring LRP onset latency differences. Psychophysiology 35, 99–115.
Miller, J., Ulrich, R., Schwarz, W., 2009. Why jackknifing yields good latency estimates. Psychophysiology 46, 300–312.
Milner, A.D., 2017. How do the two visual streams interact with each other? Exp. Brain Res. 235 (5), 1297–1308.
Milner, A.D., Goodale, M.A., 2008. Two visual systems reviewed. Neuropsychologia 46, 774–785.
Mordkoff, T.J., Gianaros, P.J., 2000. Detecting the onset of the lateralized readiness potential: a comparison of available methods and procedures. Psychophysiology 37, 347–360.
Muggeo, V.M.R., 2008. Segmented: an R package to fit regression models with broken-line relationships. R News 8, 20–25.
Murata, A., Fadiga, L., Fogassi, L., Gallese, V., Raos, V., Rizzolatti, G., 1997. Object representation in the ventral premotor cortex (area F5) of the monkey. J. Neurophysiol. 78, 2226–2230.
Nuwer, M.R., Comi, G., Emerson, R., Fuglsang-Frederiksen, A., Guérit, J.M., Hinrichs, H., et al., 1998. IFCN standards for digital recording of clinical EEG. Electroencephalogr. Clin. Neurophysiol. 106, 259–261. doi:10.1016/s0013-4694(97)00106-5.
Osborne, J., 2010. Improving your data transformations: applying the Box-Cox transformation. Pract. Assess. Res. Eval. 15 (12).
Osman, A., Bashore, T.R., Coles, M.G., Donchin, E., Meyer, D.E., 1992. On the transmission of partial information: inferences from movement-related brain potentials. J. Exp. Psychol. Hum. Percept. Perform. 18, 217–232.
J. Pinheiro D. Bates S. DebRoy D. Sarkar R Core Team Nlme: linear and nonlinear mixed effects models. R package version 3.1-131URLhttps://CRAN.R-project.org/package=nlme2017
Pisu, V., Uccelli, S., Riggio, L., Bruno, N., 2020. Action preparation in grasping reveals generalization of precision between implicit and explicit motor processes. Neuropsychologia 141, 107406. https://doi.org/10.1016/j.neuropsychologia.2020.107406.
Roche, K., Chainay, H., 2013. Visually guided grasping of common objects: effects of priming. Vis. Cogn. 21 (8), 1010–1032.
Schenk, T., Hesse, C., 2018. Do we have distinct systems for immediate and delayed actions? A selective review on the role of visual memory in action. Cortex 98, 228–248.
Schenk, T., Franz, V.H., Bruno, N., 2011. Vision-for-perception and vision-for-action: which model is compatible with the available psycho-physical and neuropsychological data? Vis. Res. 51, 812–818.
Schwarzenau, P., Falkenstein, M., Hoorman, J., Hohsbein, J., 1998. A new method for the estimation of the onset of the lateralized readiness potential (LRP). Behav. Res. Methods. Instrum. Comput. 30, 110–117.
Seegelke, C., Güldenpenning, I., Dettling, J., Schack, T., 2016. Visuomotor priming of action preparation and motor programming is similar in visually guided and memory-guided actions. Neuropsychologia 91, 1–8.
Segalowitz, S.J., Dywan, J., Unsal, A., 1997. Attentional factors in response time variability after traumatic brain injury: an ERP study. J. Int. Neuropsychol. Soc. 3, 95–107.
Smeets, J.B.J., van der Kooij, K., Brenner, E., 2019. A review of grasping as the movements of digits in space. J. Neurophysiol. 122 (4), 1578–1597. https://doi.org/10.1152/jn.00123.2019.
Smulders, F.T.Y., Miller, J.O., 2012. The lateralized readiness potential. In: Luck, S.J., Kappenman, E.S. (Eds.), Oxford Handbook of Event-Related Potential Components. Oxford University Press, New York.
Steiger, J.H., 2004. Beyond the F test: effect size confidence intervals and tests of close fit in the analysis of variance and contrast analysis. Psychol. Methods 9 (2), 164–182.
Sutton, S., Braren, M., Zubin, J., John, E.R., 1965. Evoked-potential correlates of stimulus uncertainty. Science 150, 1187–1188.
Tucker, M., Ellis, R., 1998. On the relations between seen objects and components of potential actions. J. Exp. Psychol. Hum. Percept. Perform. 24, 830–846.
Tucker, M., Ellis, R., 2004. Action priming by briefly presented objects. Acta Psychol. 116 (2), 185–203.
Uccelli, S., Pisu, V., Riggio, L., Bruno, N., 2019. The Uznadze illusion reveals similar effects of relative size on perception and action. Exp. Brain Res. 237 (4), 953–965.
Ulrich, R., Miller, J., 2001. Using the jackknife-based scoring method for measuring LRP onset effects in factorial designs. Psychophysiology 38, 816–827.
Uznadze, D., 1966. The Psychology of Set. Consultants bureau, New York.
Verleger, R., 1997. On the utility of P3 latency as an index of mental chronometry. Psychophysiology 34, 131–156.
Westwood, D.A., Goodale, M.A., 2003. Perceptual illusion and the real-time control of action. Spat. Vis. 16, 243–254.
Westwood, D.A., Chapman, C.D., Roy, E.A., 2000. Pantomimed movements are controlled by the ventral visual stream. Exp. Brain Res. 130, 545–548.
B. Winter Linear Models and Linear Mixed Effects Models in R With Linguistic Applications https://arxiv.org/abs/1308.5499:2013 Cornell University Library
de Wit, M.M., de Vries, S., van der Kamp, J., Withagen, R., 2017. Affordances and neuroscience: steps towards a successful marriage. Neurosci. Biobehav. Rev. 80, 622–629.